UNIVERSITÀ
DEGLI STUDI
DI PADOVA

DIPARTIMENTO
DI INGEGNERIA
DELL'INFORMAZIONE

DIPARTIMENTO DI INGEGNERIA DELL'INFORMAZIONE

CORSO DI LAUREA MAGISTRALE IN BIOINGEGNERIA

"RADIOMICS ANALYSIS OF STRIATAL FDOPA PET IMAGING IN PATIENTS WITH PSYCHOSIS"

Laureanda: Astrid Schiulaz

Relatore: Prof. Mattia Veronese

Correlatore: Dott. Giovanna Nordio

ANNO ACCADEMICO 2022–2023

13/07/2023

Abstract

Purpose Schizophrenia is a debilitating psychiatric disorder characterized by an abnormal dopamine production. Right now, there is a lack of quantifiable biomarkers applied in its diagnosis and no way other than empirically to determine the patient's response to standard antipsychotic treatment. Radiomics is an image analysis technique which allows to analyze patterns not recognizable by the human eye, that may be of help for the creation of more reliable biomarkers.

Methods Radiomics features were extracted from ^{18}F-DOPA PET scans of the striatal area and compared between patients and controls first, responders to standard treatment and non-responders second. The dataset consisted in 141 healthy controls and 137 patients (71 responders, 64 non-responders). Features were extracted from the SUVr signal using MIRP. Reproducibility analysis was conducted on separate test-retest scans and an ICC = 0.80 was applied as a threshold on the computed features. The remaining features were grouped using hierarchical clustering based on Spearman correlation. ANOVA testing was conducted on the two groups.

Results 15 features were selected. Linear regression showed an influence of gender and age on most features in patients. No difference was found between patients and controls. 10 features were significantly different between responders and non-responders. The feature with the highest area under the curve was the joint maximum (AUC = 0.66). Stepwise logistic regression did not show any improved performance using the combined features.

Discussion This study seems to confirm the influence of gender and age on the development of the disease. No difference was found between controls and patients, but patients came from a dataset too heterogenous. The differences between responders and non-responders seem to highlight that in responders the dopamine production is higher and creates a more irregular signal. Joint maximum was able to differentiate between responders and non-responders better than the SUVr mean, which is what is currently used in clinical practice. Validation on an independent cohort and the use of more complex classification algorithms may improve the results.

Conclusion Radiomics features may be a support for the creation of a biomarker able to predict treatment response in psychotic patients.

Chapter 1

Introduction

1.1 Schizophrenia

Schizophrenia is a debilitating psychiatric disorder which affects approximately 1% of the global population. More than 50% of the diagnosed individuals present intermittent but long-term psychiatric problems, and around 20% of them are affected by chronic symptoms. [1] The severity of these symptoms often causes issues related to the independence of patients and the way they interact with the social environment: as a result, around 25% of patients suffer from clinical depression, substance abuse and have a higher risk of suicide. [2]

The disease is related to a broad number of symptoms which present themselves in different ways in each individual, but can essentially be divided into three categories: positive symptoms, negative symptoms and cognitive impairment.

Positive symptoms are also common to every form of psychosis and include delusions, hallucinations and disorganized thoughts and speech. They tend to relapse and remit, while the other types of symptoms are usually chronic. [3]

Negative symptoms are characterized by the lack of normal emotional responses and thought processes: they include forms of apathy and diminished verbal and non-verbal expression. [3]

The cognitive impairment affects multiple domains (executive function, attention/vigilance, working memory, verbal fluency, visuospatial skills,

processing speed, and social cognition) and appears in nearly four out of five individuals who suffer from schizophrenia. [4]

The disease is equally present in men and women, although usually the onset appears later in the female population: the first episode of psychosis usually happens between the late teens and the early twenties in men, and around the mid-twenties and early thirties in women. [5] The onset can be sudden without any previous episode, although it is common to observe a prodromal stage in around 75% of the patients, during which the first symptoms develop and dysfunctions in cognitive abilities or social withdrawals may be observed. [6]

Right now, there is no certainty regarding the causes of the development of this disease. Many studies have found a genetic disposition in patients affected by schizophrenia, [7] however a specific gene related to the disease does not seem to exist, and it is more likely that more genetic loci, each one with a small effect, determine the risk that the individual will develop schizophrenia. [8]

While genetic disposition plays a role, it has also been observed that the presence of specific environmental factors during several stages of the individual's development has an influence on the possibility of the appearance of psychotic symptoms. These factors have cumulative/additive effects, which makes it likely that schizophrenia is a product of the interaction of the genetic factors and environmental ones. [7] Several studies have been conducted during this phase, searching for proper biomarkers from different points of view (structural and functional brain imaging, cerebrospinal fluid and blood analysis): the results seem to indicate that, while there are some promising findings, complex multimodal models which integrate different kinds of information are needed to properly understand this stage. [9]

The underlying mechanisms of the disease are unknown, and right now there are no anatomical or functional alterations in the brain which have been observed in subjects with schizophrenia only. [10]

At the moment, the prominent hypotheses are related to the dopaminergic and glutamatergic dysfunction which have been consistently observed in schizophrenic patients, [11] [12] [13] although the exact correlation between these abnormalities and the presence of symptoms is not well understood.

1.2 The dopamine hypothesis

Dopamine is a neurotransmitter involved in several brain pathways, playing a role in motor control, motivation, reward, cognitive function, maternal, and reproductive behaviors. [14] Its structure is depicted in Figure 1.1.

It has been repeatedly observed that presynaptic dopamine synthesis and release is altered in patients with schizophrenia, especially in the striatum. [10]

This was firstly hypothesized after observing that administering compounds which increase the extracellular concentrations of dopamine creates symptoms similar to those observed in schizophrenia. [15] Additionally, drugs which reduce dopamine levels show a reduction of psychotic symptoms, [16] [17] and a connection exists between their clinical effectiveness and the affinity with dopamine receptors. [18] [19]

Both post-mortem and *in vivo* studies have identified abnormalities in the presynaptic and post-synaptic system in patients with schizophrenia, [20] with a focus on D2 receptors, which are the main targets of antipsychotic drugs.

The link between the dopamine alteration and the psychotic symptoms however is not perfectly clear, and different theories have been proposed. [21]

Since it has been observed that midbrain dopamine neurons are activated by unexpected salient events, the dopamine alterations present in the brain may cause an attribution of importance to irrelevant stimuli, causing the onset of psychosis. [22]

Additionally, the striatum works as an integrative hub which works as a moderator between the limbic and motor regions [23]: the aberrant dopamine signaling may create a noise which is the cause of the impairments observed in schizophrenia by disrupting the integration of cortical inputs. [20] [24]

The striatum is also involved in pathways related to motor signals responsible for making the individual understand that a specific motor act is self-authored and not caused by an external agent [25] (called *efference copies*), and dopamine alterations may disrupt those signals and contribute to the feeling of passivity reported by schizophrenic patients. [20]

There are also studies which suggest that increased striatal dopamine signaling leads to negative symptoms, which may be related to impaired reward-based learning. [26] [27]

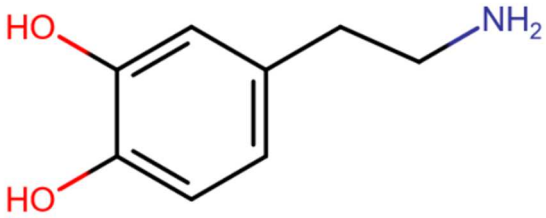

Figure 1.1: Dopamine structure

It must however be noted that the abnormalities observed in the dopamine system are not able to fully explain the symptoms observed in patients, and a direction of causality has not been determined yet. One of the main limitations to this hypothesis is the response to currently available antipsychotics: while it is true that their administration is generally followed by a decrease in the psychotic symptoms, around one third of patients does not respond to this medication [28] and need to turn to clozapine treatment, which is a stronger antipsychotic with significant side effects.

It appears that patients not responding to standard antipsychotic medications show a significantly lower dopamine synthesis capacity compared to responders, [29] which may indicate the existence of sub-types of schizophrenia which happen with different modalities.

1.3 ^{18}F-DOPA

l-6-[^{18}F]fluoro-3,4-dihydroxyphenylalanine is a radiotracer used in combination to PET imaging to quantify the dopaminergic presynaptic function. It is labelled with the isotope fluorine-18 (^{18}F) and has a half-life of 110 minutes. [30] The compound is actively transported through the blood-brain barrier, after entering the cells the aromatic amino acid decarboxylase enzyme (AADC) transforms l-DOPA into dopamine, which is stored in presynaptic vesicles and is then

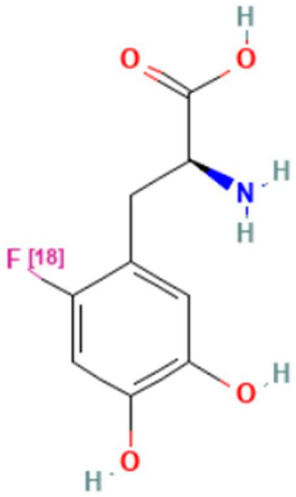

Figure 1.2: [18]F-DOPA structure [35]

released during neurotransmission. [31]

Its structure is depicted in Figure 1.2.

FDOPA has previously shown potential to be used as a biomarker to differentiate between schizophrenic patients and healthy subjects, [32] as well as between responders and non-responders to antipsychotic treatment. [33]

Furthermore, the compound produces a signal that has shown high test-retest reproducibility, especially regarding the striatal area, [34] which makes it a perfect tool to investigate dopaminergic signaling in schizophrenia.

1.4 Radiomics

Radiomics is an image analysis technique which extracts quantitative features from diagnostic measures. Radiomics features can describe imaging patterns relative to tissue properties that may be difficult to notice by human eye alone. These features are related to the intensity of the voxels in an image, with a focus on the roughness of the texture and the heterogeneity of the signal.

Official guidelines for radiomics feature extraction have been defined by the Image Biomarker Standardization Initiative (IBSI), [36] which has defined 11 feature classes for a total of 169 features, along with digital phantoms to assess

the accuracy of the software used for feature extraction. [37]

To get a general idea, radiomics features can be divided in histogram-based, texture-based, shape-based, transform-based and model-based. [38]

Histogram-based features are derived from the intensity histogram of the image and based on the single voxels, while texture-based features caption specific relationships between voxels, reflecting the eventual presence of spatial patterns or the uniformity of the texture.

Shape-based features describe the geometrical aspects of the region of interest, while the last two categories are currently still being defined by IBSI and are of no interest for this study.

Radiomics can be applied to several imaging modalities, both in 2D and 3D, and may be used to capture tissue and lesion properties, making it of particular interest in oncology. [38] This is because these features better allow to capture the heterogeneity in a specific area, which in the case of tumors has been proved to be linked to survival rates, [39] and offer a wider view compared to a biopsy, which focuses only on a selected portion of cells.

Usually, a large number of features is extracted and then machine learning techniques are applied: radiomics data are mineable, making them optimal to discover unknown markers and patterns in a disease. [38]

In fact, it has been shown that radiomics is capable to successfully predict clinical endpoints, [40] response to treatment, [41] tumor staging. [42]

1.5 Purpose of the study

The need for objective, quantifiable biomarkers capable of providing biological insight into the pathophysiology of schizophrenia is evident and urgent. Furthermore, currently in clinical practice there is no way to determine if a patient will respond to standard antipsychotics other than empirically, which leads to long delays before the patient is able to undergo clozapine treatment. [43]

This study aims to apply radiomics tools to a dataset of FDOPA PET imaging to investigate brain alterations of dopamine synthesis capacity in patients with schizophrenia.

By combining the specificity of FDOPA PET signal to dopamine system and the

ability of radiomics to unveil imaging patterns not recognizable by the human eye, we hypothesized that radiomics features may highlight new aspects of this disease and be used as a tool for classification.

Specifically, we will investigate to which degree FDOPA PET radiomics is capable of identifying significant differences between patients and controls.

Moreover, we will evaluate whether FDOPA PET radiomics may be a useful tool in the prediction of the patient's response to antipsychotics.

Due to its high signal uptake and interlink with the disease, striatum is chosen as the main region of interest for radiomics analysis.

Interestingly, while some radiomics studies have been conducted on schizophrenia, [44] [45] none of them focused on dopamine synthesis nor on the striatum: given the small amount of research currently available, additional investigation may be able to highlight previously unknown aspects of this disease and determine whether this may be a promising direction in medical research.

Chapter 2

Methods

2.1 Dataset

Data used for this study came from the institutional FDOPA PET data repository available at the Institute of Psychiatry Psychology and Neuroscience (IoPPN) at King's College London. [46] A total of six studies were used, collected from three scanning sites and five different scanners.

A total of 278 scans were available for the study, composed of 141 healthy controls (82 males and 59 females, age 28.47 ± 7.81 years) and 136 patients (99 males and 37 females, age 32.07 ± 10.79 years). Among the patients, 72 were classified as responders to standard antipsychotic treatment and 64 were non-responders or treatment resistant.

Clinical scores (PANSS positive, negative, general and total) were available for only a subset of patients.

Informed written consent was obtained for all the participants and the studies were conducted following the Declaration of Helsinki and Good Clinical Practice. All the research protocols for data acquisitions were approved by local ethics committees and institutional revision boards.

A summary of the available information is reported in Table 2.1, while full details about study design and participant inclusion and exclusion criteria are reported in the original reference.

Dataset	Number of controls	Patients	Responders / Non responders	Scanner	Site	Clinical variables
KCL11102x	61	First episode patients	13/12	Hi-Rez Biograph 6 CT44391	Invicro	Yes
STRATA (1+2)	n.a.	Mixed	34/28	Hi-Rez Biograph 6 CT44391 + unkown	Invicro	Yes
SK0x (1+2)	26	Chronic	12/12	Biograph 40 Truepoint	SK	No
IMANET04	12	Chronic	12/12	unknown	Imanet	No
KCL111xxx	36	n.a.	n.a.	Biograph TruePoint 6 CT45544	Invicro	n.a
IMANET - Eagerton	7	n.a	n.a	ECAT EXACT3D	Imanet	n.a.

Table 2.1: datasets used for the study

2.2 Data acquisition

Data were all acquired with the same experimental protocol and processed with the same analysis pipeline. [46]

All FDOPA PET imaging sessions were acquired with a continuous dynamic acquisition (no blood sampling), with scanning beginning with the tracer injection and lasting for 90-95 minutes. All participants received carbidopa (150 mg) and entacapone (400 mg) orally ~1 hour before imaging. The FDOPA tracer (injected dose ranging from 86.4 to 414.4 MBq) was administered by intravenous bolus injection after the acquisition of a brain CT or MRI for attenuation correction, depending on the scanner availability at each imaging site. PET data reconstruction varied across imaging sites and scanner types, but all included correction for random noise, scatter, and tissue attenuation.

2.3 Data processing

The analysis of FDOPA PET imaging data was performed using an automated analysis pipeline written in Python and integrated in XNAT and it can be described as follows. First, dynamically non-attenuated and attenuated FDOPA

PET images are inputted into the pipeline.

The non-attenuated dynamic images are motion corrected frame-to-frame to a single reference frame with a linear transformation using Statistical Parametric Mapping (SPM) realign function. [47] The motion information is then used to realign the attenuated dynamic images, which are then summed together to create a motion-corrected individual static PET image. A tracer-specific template and atlas defining the striatum and cerebellum are co-registered to each individual motion-correct static PET image, using SPM 12 (https://www.fil.ion.ucl.ac.uk/spm/). Two parameters of interest are derived from image quantification as index of dopamine synthesis capacity. From dynamic imaging, Ki (unit 1/min) is computed using the Gjedde-Patlak graphical approach [48] [49] both region-wise and voxel-wise, with the cerebellum used as the reference region.

The Standardized Uptake Value Ratio (SUVr) at 60 minutes is also calculated as the ratio of the tracer activity to that in the cerebellum.

After this process, two subjects were removed from the study as the quality of the scans was not high enough due to the presence of motion artifacts.

2.4 Feature extraction

The volume of interest (VOI) target of radiomics analysis was defined on the dynamic scans using Python. The image segmentation was based on Ki estimates since population statistics over a larger number of subjects was previously available. [50] This permitted to determine a threshold for the VOI segmentation under which the signal in the voxels was not significant due to the presence of motion artifacts.

The striatal mask was derived for each subject from the Martinez atlas (previously co-registered in subject space), [51] two binary dilations were performed and voxels with a signal under 0.007 min^{-1} were removed.

The radiomics analysis was performed on the static scans using the SUVr parametric maps.

Radiomics features were extracted using the MIRP Python package, [52] which is IBSI compliant. [53] They were computed over the whole striatal area (both

left and right hemispheres combined), therefore not taking into consideration any possible laterality of the signal.

Prior to the feature computation, each scan was re-segmented using a threshold of 1.50, which was estimated as a lower bound for the SUVr signal in the region of interest after visual inspection of the signal's distribution. This was done so that it would be possible to discretize the images with the fixed bin size method, which is usually recommended for the SUVr signal since it maintains the relationship with the original intensity scale. [37] A fixed bin size of 0.0125 was set.

Features were computed with the 3D average aggregation method. A total of 172 radiomics features were obtained.

2.5 Feature selection

A sample of 7 controls and 7 patients from two independent studies was selected to conduct a reliability analysis of the features with the purpose to select the most reproducible ones for studies regarding the striatal FDOPA PET signal. [54]

Test-retest scans were available for each subject.

As reproducibility index, the intraclass correlation coefficient (ICC) index [55] was computed separately both for controls and patients, following the formula

$$ICC(3,1) = \frac{BMS - EMS}{BMS + (k-1)EMS}$$

where BMS and EMS are the subject and error sum of squares respectively and k is the number of repeated sessions.

Only reproducible radiomics features with an ICC > 0.80 for both patients and controls were retained for the rest of the study.

Moreover, radiomics features are known to often bring redundancy in information and to generally be highly correlated. [56] This is due to the fact that many features describe the same aspect from different points of views and

are often equivalent from a mathematical perspective.

Dimensionality was reduced through hierarchical clustering based on Spearman correlation. [57] Clusters were created in order to group together features which had an absolute correlation coefficient ρ of at least 0.90.

From each cluster, the feature with the highest ICC was selected. Since two ICC indexes were available for each feature (the patients and the controls one), the lowest between the two of them was assigned to each feature and then the selection was performed on those values.

2.6 Feature harmonization

Harmonization to correct for batch effects was applied directly to the selected features. [58]

Combat is a statistical approach which assumes the presence of site-specific shift and scaling factors, which are estimated using empirical Bayes. [59] It is possible to preserve the contribution of specific biological covariates to the data, which need to be identified priorly to the harmonization step. [60]

For this study the NeuroCombat function from the NeuroCombat python library version 0.2.10+ (https://github.com/Jfortin1/neuroCombat) was employed. Harmonization was performed separately for controls and patients, using the same reference scanner.

The effects of age and sex as covariates were preserved.

Comparison of the distribution of the complexity feature across scanners before and after harmonization is depicted in Figure 2.1.

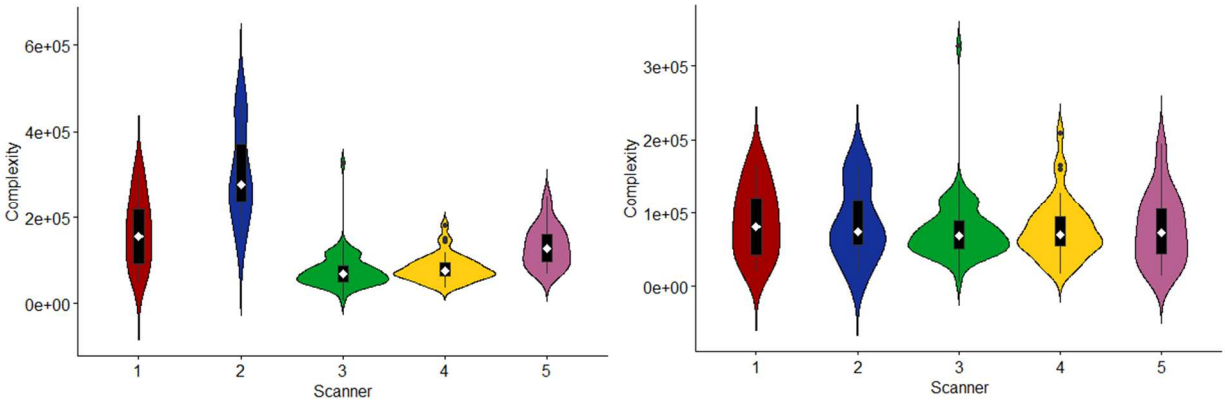

Figure 2.1: Complexity feature in the different scanners before and after harmonization in controls group

2.7 Statistical analysis

All statistical tests were performed in Matlab.

Groups were compared with the χ^2 test for categorical variables and the Wilcoxon test for continuous variables.

Regression analysis was performed in order to evaluate the influence of biological variables on the computed features.

Statistical differences between the features in patients and controls were evaluated with the ANOVA test, taking into consideration gender and age effect and corrected according to the False Discovery Rate (FDR) method. Area under the curve (AUC) was computed for all the features which resulted significantly different to analyze their performance.

The same statistical analysis was done to evaluate differences between responders and non-responders.

Chapter 3

Results

3.1 Feature selection

A total of 146 features survived the reproducibility selection in the patients' group, while 85 features survived in the controls. Only features with an ICC > 0.80 in both groups were further considered. In the end, 81 features out of 172 resulted reproducible in both groups.

These features were hence grouped in clusters based on the Spearman correlation index.

This resulted in 15 clusters, from each one of them the feature with the highest ICC was selected.

The features selected are reported in Table 3.1 along with their physiological meaning.

Feature class	Feature	Meaning
Intensity-based statistical features	Intensity-based quartile coefficient of dispersion	Measure of the dispersion of grey levels
	Median absolute deviation	Measure of the dispersion from the sample median
Neighbourhood grey tone difference based features	Complexity	Quantification of the non-uniformity of the texture and rapid changes in grey levels
Morphological features	PCA elongation	Ratio of the major and minor principal axis lengths (eccentricity of the ROI)
	Diameter	Distance between the two most distant vertices
	PCA flatness	Ratio of the major and least axis lengths (flatness of the volume relative to its length)
	PCA major axis length	Length of the major axis associated with the highest eigenvalue
Grey level size zone based features	Zone size entropy	Quantity of information contained in a matrix where the element s_{ij} = the number of zones with grey level i and size j
Grey level co-occurrence based features	Joint maximum	Most common grey level co-occurence
	Contrast	Measure of grey level variations
	Energy	Energy of the probability distribution of grey level co-occurences
Grey level distance zone based features	Zone distance non uniformity	Measure of the distribution of the number of zones over the different distances
Intensity histogram features	Median	Median value of the histogram
Grey level run length based features	Run lenght non-uniformity	Distribution of runs over the run lengths
Neighbouring grey level dependence based features	Low dependence low grey level emphasis	Emphasis on the number of groups with a low number of voxels centered on a low grey level voxel

Table 3.1: Reproducible features selected for each cluster: definition and meaning

3.2 Controls – patients comparison

Study population

Outliers were identified by applying a threshold of mean ±3 σ to each radiomics feature by considering the full data sample. Two subjects were found to be outliers in more than three features and were therefore removed from the study. The remaining subjects were 273, 138 controls and 135 patients. The two groups were unmatched both in terms of gender (χ^2 test, $p = 0.011$) and age (Wilcoxon rank sum test, $p = 0.013$).

A summary of the demographic of the dataset, along with the results of the statistical analyses, is available in table 3.2.

	Controls	Patients	p-value
Gender (male/female)	80/58	98/37	0.011
Age	28.5 ± 7.9	32.0 ± 10.8	0.013
Total	138	135	

Table 3.2: gender and age distribution in controls and patients, along with the p-values obtained after χ^2 and Wilcoxon testing

Linear regression analysis

A linear regression model using gender and age was computed for each feature to check for the eventual influence of the two covariates.

In the controls group, 4 features (the morphological ones) were significantly related to gender and 2 related to age. In the patients, 12 features were significantly influenced by gender, and 6 by age.

The significant p-values of the regression analysis, after being adjusted according to FDR correction, are reported in table 3.3. An example is reported in Figure 2.1, where the complexity feature is plotted against age in controls and patients and a regression line is plotted for each gender.

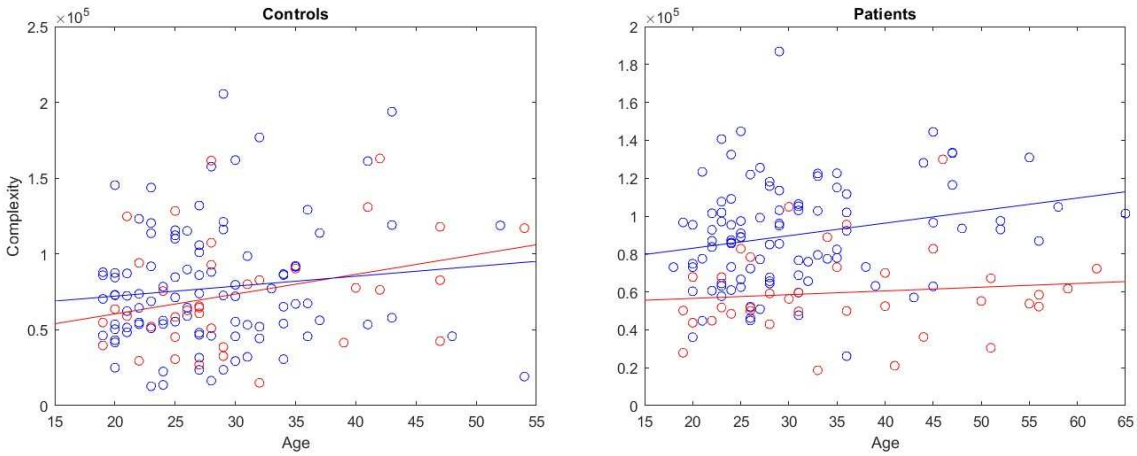

Figure 3.1: Complexity feature plotted against age in controls and patients. A regression line is plotted for males (blue) and women (red)

	Controls		Patients	
Feature	Gender	Age	Gender	Age
Coefficient of dispersion				
Complexity			<0.001	0.032
PCA elongation	0.036			<0.001
Diameter	<0.001	0.048	<0.001	
Zone size entropy			<0.001	
Joint maximum			0.026	
Zone distance non uniformity			<0.001	0.004
Median			<0.001	
Run lenght non uniformity			0.011	0.009
Median absolute deviation			0.011	
Contrast		0.038	<0.001	0.003
PCA flatness	<0.001			0.012
PCA major axis	<0.001		<0.001	
Low dependence low grey level emphasis			<0.001	
Energy			0.012	

Table 3.3: significant adjusted p-values of the linear regression model accounting for gender and age for each feature

ANOVA analysis

ANOVA testing was performed on radiomics features to test for differences between patients and controls. Given the association of gender and age with radiomics features, they were included as covariates. After FDR correction, no features were found to significantly differentiate between the two groups.
There were differences related to gender in 7 features, and differences related to age in 5 features.
The resulting adjusted p-values are reported in Table 3.4

Feature	Group	Gender	Age
Coefficient of dispersion			
Complexity		0.014	
PCA elongation		0.022	0.008
Diameter		<0.001	
Zone size entropy			
Joint maximum			
Zone distance non uniformity		0.008	0.002
Median			
Run lenght non uniformity			0.002
Median absolute deviation			
Contrast		0.022	0.011
PCA flatness		<0.001	0.014
PCA major axis		<0.001	
Low dependence low grey level emphasis			
Energy			

Table 3.4: significant adjusted p-values after ANOVA comparison between controls and patients, taking into account gender and age

Within studies comparison

Given the observed heterogeneity between the different studies which composed the data used for this study, a separate ANOVA analysis has been conducted on each dataset separately. Three out of six studies employed both controls and patients, their demographics can be observed in table 3.5.
ANOVA was performed adding gender and age as covariates, but no significant difference was found.

	Gender (male/female)			Age		
Study	Controls	Patients	p-value	Controls	Patients	p-value
FDOPA01 (KCL11102x)	32/26	21/4	0.039	26.5 +/- 5.6	26.2 +/- 4.4	1
FDOPA02 (SK)	16/10	17/7	0.976	26.2 +/- 7.2	31.8 +/- 9.4	0.0387
FDOPA03 (IMANET)	5/7	10/14	1	43.5 +/- 8.3	45.0 +/- 10.2	0.9936

Table 3.5: age and gender of patients and controls in the three different studies used, along with the p-values obtained from the χ^2 and Wilcoxon test

3.3 Responders – non-responders comparison

Study population

The patients group was further divided into one group composed of responders to standard antipsychotic treatment (71 subjects) and one composed of non-responders or treatment resistant patients (64 subjects). The two groups resulted matched both in gender (p = 0.480) and age (p = 0.281) after χ^2 and Wilcoxon testing.

Group's demographics, along with the results of statistical analyses, are reported in Table 3.7.

	Responders	Non Responders	p-value
Gender (male/female)	39/32	39/25	0.480
Age	31.5 ± 11.2	32.6 ± 10.5	0.281
Total	71	64	

Table 3.7: gender and age distribution in responders and non-responders, along with the p-values obtained after χ^2 and Wilcoxon testing

Correlation with clinical symptoms

PANSS score values (positive, negative, general psychopathology, total score) were available for 62 patients. Multilinear regression was performed to evaluate if there was an influence of the overall symptoms on the radiomics features, but no significant values were found. Linear regression was also performed separately for each PANSS index, but again no significant correlation was found.

ANOVA analysis

A total of 10 features resulted significantly different between the two groups after FDR correction. Differences due to gender and age were present in a large amount of features (13 and 6 respectively). Significant adjusted p-values are reported in table 3.8. The distribution of the 10 features is plotted in Figure 3.2.

Feature	Group	Gender	Age
Coefficient of dispersion	0.004	0.048	
Complexity		<0.001	0.030
PCA elongation	0.049		0.002
Diameter		<0.001	
Zone size entropy	0.021	0.001	
Joint maximum	0.003	0.021	
Zone distance non uniformity	0.017	<0.001	0.009
Median	0.021	<0.001	
Run lenght non uniformity	0.027	0.014	0.017
Median absolute deviation	0.014	0.002	
Contrast	0.049	<0.001	0.004
PCA flatness			0.021
PCA major axis		<0.001	
Low dependence low grey level emphasis		0.002	
Energy	0.014	0.014	

Table 3.8: significant adjusted p-values after ANOVA testing between responders and non-responders

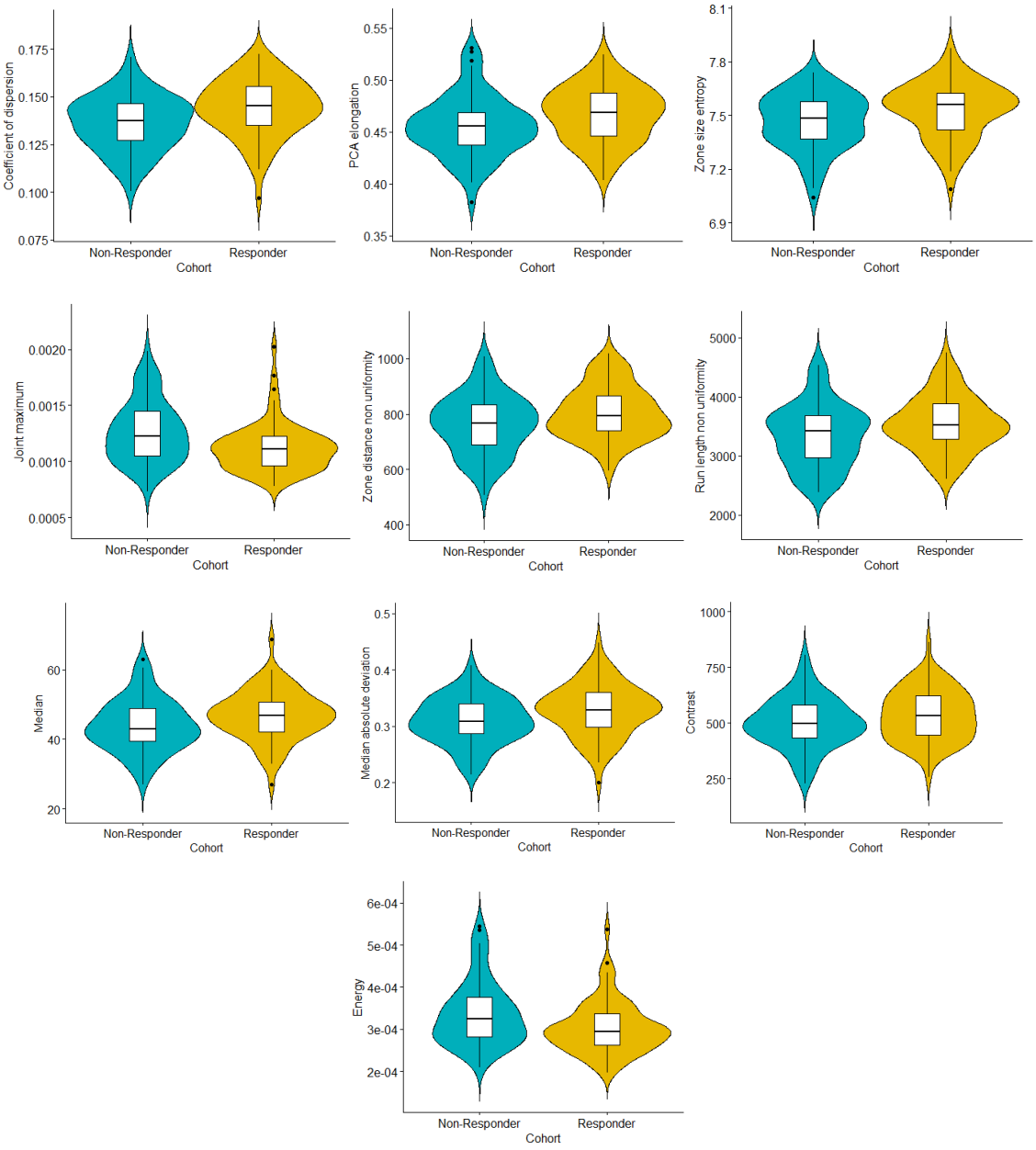

Figure 3.2: distribution of the features which resulted significantly different between responders and non-responders

Area under the curve performance

The p-values from ANOVA tests and AUC observed for each significant feature are reported in Table 3.9. The feature with the highest value was the joint maximum, with an AUC = 0.66, which is higher than the one from SUVr mean (AUC = 0.61). The two ROC curves are plotted in Figure 3.3. The other features had similar values.

Feature	p-value	AUC
Coefficient of dispersion	0.004	0.656
PCA elongation	0.049	0.623
Zone size entropy	0.021	0.616
Joint maximum	0.003	0.661
Zone distance non uniformity	0.017	0.601
Median	0.021	0.625
Run lenght non uniformity	0.027	0.607
Median absolute deviation	0.014	0.628
Contrast	0.049	0.576
Energy	0.014	0.623

Table 3.9: p-value of ANOVA test and area under the curve for each significant feature

Stepwise logistic regression

An additional stepwise logistic regression was performed using all the significant features to see if their combined performance may improve the results. Only the joint maximum was the one which was found to add significant value to the regression model, with $p < 0.001$.

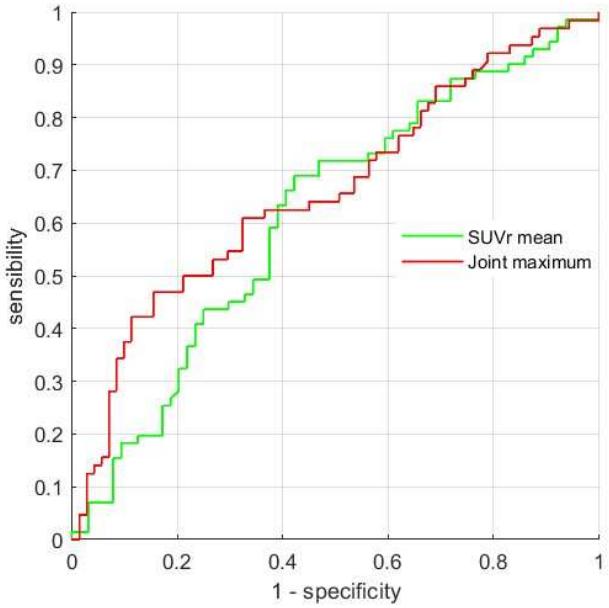

Figure 3.3: comparison of ROC curve performance of SUVr mean and joint maximum in differentiating between responders and non-responders

Within studies comparison

Given the observed heterogeneity between the different datasets used, a separate ANOVA analysis has been conducted within each one of them. Four out of six datasets contained psychotic subjects. In each study, responders and non-responders were matched both in gender and age. The demographics for each dataset are reported in Table 3.10.

The significant adjusted p-values are reported in Table 3.11.

Except for FDOPA04, a large number of radiomics features were shown to be significantly different between the two groups. They were generally the same features which were shown to differentiate between the two groups on the ANOVA analysis of the whole dataset.

	Gender (male/female)			Age		
Study	Responders	Non responders	p-value	Responders	Non responders	p-value
FDOPA01 (KCL1102x)	10/3	11/1	0.315	24.9 +/- 3.0	27.6 +/- 5.4	0.249
FDOPA02 (SK)	8/4	9/3	0.653	32.3 +/- 10.8	31.3 +/- 8.1	0.885
FDOPA03 (IMANET)	6/6	4/8	0.408	44.0 +/- 11.9	46.1 +/- 10.2	0.643
FDOPA04 (STRATA)	27/7	23/5	0.786	29.4 +/- 9.8	29.5 +/- 8.6	0.655

Table 3.10: gender and age distribution of responders and non-responders cohorts in each study, along with the p-values obtained after statistical comparison

Feature	**FDOPA01** (KCL11102z)	**FDOPA02** (SK)	**FDOPA03** (IMANET)	**FDOPA04** (STRATA)
Coefficient of dispersion	0.007	0.040	0.007	
Complexity	0.044		0.010	
PCA elongation			0.019	
Diameter				
Zone size entropy		0.045	0.003	
Joint maximum	0.007	0.038	0.002	
Zone distance non uniformity	0.018		0.020	
Median		0.045	0.005	
Run lenght non uniformity	0.007		0.005	
Median absolute deviation	0.018	0.045	0.005	
Contrast			0.014	
PCA flatness			0.003	
PCA major axis			0.040	
Low dependence low grey level emphasis			0.007	
Energy	0.018	0.045	0.003	

Table 3.11: adjusted p-values after ANOVA testing within the different datasets between responders and non-responders groups

Chapter 4

Discussion

This study extracted radiomics features from FDOPA PET scans of the striatal area in schizophrenic patients and healthy controls. While no consistent differences were found between patients and healthy controls, ten out of the fifteen most reproducible features resulted significantly different between patients responding to standard treatment and non-responders. In particular, the joint maximum was the feature which showed the highest classification accuracy, indicating that values related to striatal dopamine production are informative for prediction of treatment response in psychosis.

Covariates analysis

Our covariate analysis of radiomics features showed that gender and age were associated with data obtained from patients, much less with controls.
In controls, gender turned out to be related only to the morphological features, which describe the geometrical properties of the region of interest, in this case the striatum.
This might be explained by anatomical properties of the area, as the striatum tends to be smaller in women. [61] A minor influence of age was observed, as it resulted significant in only two features, but it is not enough to argue that it has a significant influence on dopamine signaling.
There was a bit of uncertainty whether to include morphological features in the cross-sectional analysis: many of these measures are related to the sphericity of the region of interest, which are directly linked to the aggressiveness of the tumor, but of little importance when measuring the striatum.
It does however seem that some changes in the morphology of this area appear in schizophrenic patients. While there are different opinions regarding the presence of a volume difference in patients compared to controls, [62] [63] changes in shape do exist [64] and may also be influenced by the assumption of

medication. [65] While it is not certain that morphological features may be able to capture these variations in a significant way, there was no reason to exclude them from this analysis.

Furthermore, the region of interest was extracted using the FDOPA PET signal, which quantifies dopamine production. While the production is concentrated in the striatal area, it may be more or less extended depending on the presence of the disease. It must also be noted that the selected morphological features do not penalize the information that may have been otherwise brought by other features, since features were selected through clustering based on correlation.

The situation is different in patients, where a large group of features was influenced both by gender and age. There currently is some evidence that gender causes differences in cognitive functions and neuroanatomy in patients with schizophrenia, but the findings are not consistent enough. [66] [67] It is however known for certainty that the age at which the first psychotic symptoms appear varies between men and women [64], and these findings seem to support the hypothesis that it has an influence on other aspects of the disease as well.

Among the morphological features, two do no result significantly different in the patients group, which was expected given the results in the controls. They are features which quantify the eccentricity and the flatness of the ROI, which are therefore not directly linked to its volume, so this may be why they did not show any gender-based difference, or it may be due to sample bias.

Age has been shown to be related to cognitive changes in schizophrenic patients different than those observed in a healthy population, [68] so it may influence other aspects of the disease as well.

These findings seem to confirm that both these factors play a role in the development of schizophrenia, and possibly in the abnormalities observed in dopamine production.

Cross-sectional analysis

ANOVA testing showed that there were differences in the radiomics features between patients and controls which were due to gender and age, but none of them was able to differentiate between the two groups.

No literature exists right now to compare these results to, since none of the

radiomics studies on schizophrenia focused on PET imaging related to dopamine production.

These results may be partially explained by the fact that there was a lot of heterogeneity between the patients enrolled for this study: data came from several datasets, which were composed of subjects at different stages of the treatment and the development of the disease. Treatment does influence the dopamine production, since the D_2 occupancy increases after antipsychotic assumption, [69] and may therefore cause too much variation among the signal measured from patients.

The study may benefit by focusing on a more clinically homogeneous group, ideally unmedicated.

For this reason, an additional ANOVA analysis was conducted separately on each dataset, with however poor results: no difference due to group, gender or age was found. This may be a further indicator that the differences previously found were only related to the heterogeneity of the datasets, but it must also be taken into consideration that few subjects (from 83 to 36) were available for each dataset, which makes the results of inferential statistics less powered.

Except for the morphological features, the majority of the radiomics features selected focused on the distribution of the signal in the region of interest. The results seem to imply that, although it is known that there are abnormalities in dopamine production in patients, there is no substantial difference in the distribution or uniformity of the signal in one group or the other. The unexpected result was the median, since the signal was expected to be higher in patients.

It must however be noted that usually these comparisons are made by differentiating between responders and non-responders, as there are important differences between the two groups that cannot be overlooked.

ANOVA testing between controls and non-responders did not reveal any difference, which is to be expected given that dopamine production in non-responders should be close to the normal range.

There were however differences with the responders, which did not survive FDR correction. The number of analyzed features was particularly high and many tests were performed, therefore further feature reduction in order to focus only on few important aspects could give different results and highlight some of the differences observed before FDR.

Analysis of treatment response

In the responders – non-responders comparison, ten out of fifteen features resulted to be significantly different between the two groups, with an influence of gender and age always present.

From a visual inspection, it can be observed that generally responders have higher values than non-responders. The majority of features are related to the irregularity of the analyzed texture, which means that in responders the distribution of the signal is more irregular and less uniform. The fact that the median of the signal is also higher implies that in these individuals there is more dopamine production, therefore there is more activity in the striatal area which creates more irregularities in the patterns created by the signal.

The elongation of the region of interest is also higher. A value close to 1 reflects a sphere-like shape, while lower values express a greater elongation in the ROI. As previously stated, there seems to be an effect of medications on the brain's anatomy, but the findings are not consistent enough. It could also be argued that this difference is caused by the increased dopaminergic activity, which may change the extension of the area. There is however no difference in the other morphological features.

The only two features where the non-responders had higher values were the joint maximum and the energy, which both belong to the grey level co-occurrence class. Features in this class are computed after creating a matrix which represents the number of occurrences of two consecutive voxels with a set grey level in a direction, to put it simply it reports how many times a voxel with grey level x is followed by a voxel with grey level y. The probability to observe a certain co-occurrence can then be extracted from the matrix, from which the energy of the probability distribution can be computed. The joint maximum is the probability corresponding to the most common co-occurrence observed. The fact that both these values are higher in non-responders means that there are higher probabilities to observe specific co-occurrences, which means that there is a more regular pattern in the distribution of the signal. Again, this is related to the fact that the higher activity in responders causes more heterogeneity in the signal's distribution.

These differences seem to carry on when analyzing each dataset separately, and are therefore not dependent on the clinical state of the patients, except for the

FDOPA04 group. The group however was composed of subjects who did not take medication as regularly as they should have.
While the features are different between the two groups, the performance of the AUC is relatively poor.
Stepwise regression was performed to observe if the combined features may improve the performance, but only joint maximum significantly improved the model. This may be caused by the high correlation between the features, which therefore brings a lot of redundancy in information. However, more complex classification algorithms may still improve these results.
Still, joint maximum gave a better result than the SUVr mean in differentiating between the two groups (AUC = 0.61), which is the index that right now is mostly implemented in clinical practice. The mean of the signal was not one of the fifteen features used for the study, but it was located in the cluster from which the median was selected.

Limitations

This study had some limitations. As mentioned, the dataset utilized had heterogeneity issues. Patients went from first-episode schizophrenia to chronic situations, which may have caused some inconsistency in the findings.
The study may also improve with a major number of subjects, so that validation of the results on an independent cohort may be possible.
We are also aware of the limitations radiomics brings. Its major issue is related to the reproducibility of findings, since the computation of the features is heavily dependent on many factors such as the imaging modality, the discretization method, the segmentation. [70]
The process of feature selection was repeated on the test-retest scans with a lower number of grey levels, but the results did not change significantly: the majority of the selected features remained the same, and the few which changed maintained such a high correlation index with the not-selected ones that it is safe to assume that no information was lost. The features also had high correlation indexes with the ones used for the study.

Conclusion

This study showed that radiomics features highlight significant differences between schizophrenic patients who respond to standard antipsychotic treatment and those who do not. In particular, the joint maximum feature had the highest performance in differentiating between the two groups, with an increase compared to the SUVr signal mean, which is what is currently employed in clinical studies.

Future studies on a larger dataset with more complex classification models may highly improve the current situation. Radiomics features may be a potential support for the creation of a biomarker to early identify responders to antipsychotic treatment, and improve the understanding of the underlying biology of the disease.

Bibliography

1. Owen MJ, Sawa A, Mortensen PB. Schizophrenia. Lancet. 2016 Jul 2;388(10039):86-97. doi: 10.1016/S0140-6736(15)01121-6. Epub 2016 Jan 15. PMID: 26777917; PMCID: PMC4940219.

2. Jablensky A., Sartorius N., Ernberg G., Anker M., Korten A., Cooper J.E., Day R., Bertelsen A. Schizophrenia: Manifestations, incidence and course in different cultures. A World Health Organization ten-country study. Psychol. Med. Monogr. Suppl. 1992;20:1–97. doi: 10.1017/S0264180100000904.

3. Batinic B. Cognitive Models of Positive and Negative Symptoms of Schizophrenia and Implications for Treatment. Psychiatr Danub. 2019 Jun;31(Suppl 2):181-184. PMID: 31158119.

4. Kar SK, Jain M. Current understandings about cognition and the neurobiological correlates in schizophrenia. J Neurosci Rural Pract. 2016 Jul-Sep;7(3):412-8. doi: 10.4103/0976-3147.176185. PMID: 27365960; PMCID: PMC4898111.

5. Schultz SH, North SW, Shields CG. Schizophrenia: a review. Am Fam Physician. 2007 Jun 15;75(12):1821-9. PMID: 17619525.

6. George M, Maheshwari S, Chandran S, Manohar JS, Sathyanarayana Rao TS. Understanding the schizophrenia prodrome. Indian J Psychiatry. 2017 Oct-Dec;59(4):505-509. doi: 10.4103/psychiatry.IndianJPsychiatry_464_17. PMID: 29497198; PMCID: PMC5806335.

7. Wahbeh MH, Avramopoulos D. Gene-Environment Interactions in Schizophrenia: A Literature Review. Genes (Basel). 2021 Nov 23;12(12):1850. doi: 10.3390/genes12121850. PMID: 34946799; PMCID: PMC8702084.

8. Schork AJ, Wang Y, Thompson WK, Dale AM, Andreassen OA. New statistical approaches exploit the polygenic architecture of schizophrenia--implications for the underlying neurobiology. Curr Opin Neurobiol. 2016 Feb;36:89-98. doi: 10.1016/j.conb.2015.10.008. Epub 2015 Nov 8. PMID: 26555806; PMCID: PMC5380793.

9. Goff DC, Romero K, Paul J, Mercedes Perez-Rodriguez M, Crandall D, Potkin SG. Biomarkers for drug development in early psychosis: Current issues and promising directions. Eur Neuropsychopharmacol. 2016 Jun;26(6):923-37. doi: 10.1016/j.euroneuro.2016.01.009. Epub 2016 Mar 19. PMID: 27005595.

10. Linden DE. The challenges and promise of neuroimaging in psychiatry. Neuron. 2012 Jan 12;73(1):8-22. doi: 10.1016/j.neuron.2011.12.014. PMID: 22243743.

11. Grace AA. Dysregulation of the dopamine system in the pathophysiology of schizophrenia and depression. Nat Rev Neurosci. 2016 Aug;17(8):524-32. doi: 10.1038/nrn.2016.57. Epub 2016 Jun 3. PMID: 27256556; PMCID: PMC5166560.

12. Howes OD, McCutcheon R, Owen MJ, Murray RM. The Role of Genes, Stress, and Dopamine in the Development of Schizophrenia. Biol Psychiatry. 2017 Jan 1;81(1):9-20. doi: 10.1016/j.biopsych.2016.07.014. Epub 2016 Aug 6. PMID: 27720198; PMCID: PMC5675052.

13. Uno Y, Coyle JT. Glutamate hypothesis in schizophrenia. Psychiatry Clin Neurosci. 2019 May;73(5):204-215. doi: 10.1111/pcn.12823. Epub 2019 Mar 6. PMID: 30666759.

14. Klein MO, Battagello DS, Cardoso AR, Hauser DN, Bittencourt JC, Correa RG. Dopamine: Functions, Signaling, and Association with Neurological Diseases. Cell Mol Neurobiol. 2019 Jan;39(1):31-59. doi: 10.1007/s10571-018-0632-3. Epub 2018 Nov 16. PMID: 30446950.

15. Lieberman JA, Kane JM, Alvir J. Provocative tests with psychostimulant drugs in schizophrenia. Psychopharmacology (Berl) 1987;91:415–33.

16. Carlsson A, Roos BE, Wålinder J, Skott A. Further studies on the mechanism of antipsychotic action: potentiation by alpha-methyltyrosine of thioridazine effects in chronic schizophrenics. J Neural Transm. 1973;34(2):125-32. doi: 10.1007/BF01244665. PMID: 4146641.

17. Wålinder J, Skott A, Carlsson A, Roos BE. Potentiation by metyrosine of thioridazine effects in chronic schizophrenics. A long-term trial using double-blind crossover technique. Arch Gen Psychiatry. 1976 Apr;33(4):501-5. doi: 10.1001/archpsyc.1976.01770040061011. PMID: 779704.

18. Seeman P, Lee T. Antipsychotic drugs: direct correlation between clinical potency and presynaptic action on dopamine neurons. Science. 1975 Jun 20;188(4194):1217-9. doi: 10.1126/science.1145194. PMID: 1145194.

19. Creese I, Burt DR, Snyder SH. Dopamine receptor binding predicts clinical and pharmacological potencies of antischizophrenic drugs. Science. 1976 Apr 30;192(4238):481-3. doi: 10.1126/science.3854. PMID: 3854.

20. Howes O, McCutcheon R, Stone J. Glutamate and dopamine in schizophrenia: an update for the 21st century. J Psychopharmacol. 2015 Feb;29(2):97-115. doi: 10.1177/0269881114563634. Epub 2015 Jan 13. PMID: 25586400; PMCID: PMC4902122.

21. McCutcheon RA, Abi-Dargham A, Howes OD. Schizophrenia, Dopamine and the Striatum: From Biology to Symptoms. Trends Neurosci. 2019 Mar;42(3):205-220. doi: 10.1016/j.tins.2018.12.004. Epub 2019 Jan 6. PMID: 30621912; PMCID: PMC6401206.

22. Winton-Brown TT, Fusar-Poli P, Ungless MA, Howes OD. Dopaminergic basis of salience dysregulation in psychosis. Trends Neurosci. 2014 Feb;37(2):85-94. doi: 10.1016/j.tins.2013.11.003. Epub 2014 Jan 2. PMID: 24388426.

23. Lerner TN, Shilyansky C, Davidson TJ, Evans KE, Beier KT, Zalocusky KA, Crow AK, Malenka RC, Luo L, Tomer R, Deisseroth K. Intact-Brain Analyses Reveal Distinct Information Carried by SNc Dopamine Subcircuits. Cell. 2015 Jul

30;162(3):635-47. doi: 10.1016/j.cell.2015.07.014. PMID: 26232229; PMCID: PMC4790813.

24. Kellendonk C, Simpson EH, Polan HJ, Malleret G, Vronskaya S, Winiger V, Moore H, Kandel ER. Transient and selective overexpression of dopamine D2 receptors in the striatum causes persistent abnormalities in prefrontal cortex functioning. Neuron. 2006 Feb 16;49(4):603-15. doi: 10.1016/j.neuron.2006.01.023. PMID: 16476668

25. Fee MS. The role of efference copy in striatal learning. Curr Opin Neurobiol. 2014 Apr;25:194-200. doi: 10.1016/j.conb.2014.01.012. Epub 2014 Feb 21. PMID: 24566242; PMCID: PMC4153469.

26. Gold JM, Waltz JA, Matveeva TM, Kasanova Z, Strauss GP, Herbener ES, Collins AG, Frank MJ. Negative symptoms and the failure to represent the expected reward value of actions: behavioral and computational modeling evidence. Arch Gen Psychiatry. 2012 Feb;69(2):129-38. doi: 10.1001/archgenpsychiatry.2011.1269. PMID: 22310503; PMCID: PMC4406055.

27. Maia TV, Frank MJ. An Integrative Perspective on the Role of Dopamine in Schizophrenia. Biol Psychiatry. 2017 Jan 1;81(1):52-66. doi: 10.1016/j.biopsych.2016.05.021. Epub 2016 Jun 1. PMID: 27452791; PMCID: PMC5486232.

28. Mortimer AM, Singh P, Shepherd CJ, Puthiryackal J. Clozapine for treatment-resistant schizophrenia: National Institute of Clinical Excellence (NICE) guidance in the real world. Clin Schizophr Relat Psychoses. 2010 Apr;4(1):49-55. doi: 10.3371/CSRP.4.1.4. PMID: 20643629.

29. Demjaha A, Murray RM, McGuire PK, Kapur S, Howes OD. Dopamine synthesis capacity in patients with treatment-resistant schizophrenia. Am J Psychiatry. 2012 Nov;169(11):1203-10. doi: 10.1176/appi.ajp.2012.12010144. PMID: 23034655.

30. Fluorodopa F18 (Systemic). Available at: http://www.drugs.com. Accessed April 24, 2023.

31. Chondrogiannis S, Marzola MC, Rubello D. ^{18}F-DOPA PET/computed tomography imaging. PET Clin. 2014 Jul;9(3):307-21. doi: 10.1016/j.cpet.2014.03.007. Epub 2014 Apr 29. PMID: 25030394.

32. Bose SK, Turkheimer FE, Howes OD, Mehta MA, Cunliffe R, Stokes PR, Grasby PM. Classification of schizophrenic patients and healthy controls using [18F] fluorodopa PET imaging. Schizophr Res. 2008 Dec;106(2-3):148-55. doi: 10.1016/j.schres.2008.09.011. Epub 2008 Oct 11. PMID: 18849151.

33. Veronese M, Santangelo B, Jauhar S, D'Ambrosio E, Demjaha A, Salimbeni H, Huajie J, McCrone P, Turkheimer F, Howes O. A potential biomarker for treatment stratification in psychosis: evaluation of an [^{18}F] FDOPA PET imaging approach. Neuropsychopharmacology. 2021 May;46(6):1122-1132. doi: 10.1038/s41386-020-00866-7. Epub 2020 Sep 22. PMID: 32961543; PMCID: PMC8115068.

34. Egerton A, Demjaha A, McGuire P, Mehta MA, Howes OD. The test-retest reliability of 18F-DOPA PET in assessing striatal and extrastriatal presynaptic dopaminergic function. Neuroimage. 2010 Apr 1;50(2):524-531. doi: 10.1016/j.neuroimage.2009.12.058. Epub 2009 Dec 23. PMID: 20034580; PMCID: PMC4096947.

35. National Center for Biotechnology Information (2023). PubChem Compound Summary for CID 56494, Fluorodopa (18F). Retrieved April 24, 2023 from https://pubchem.ncbi.nlm.nih.gov/compound/Fluorodopa-_18F.

36. Zwanenburg A, Vallières M, Abdalah MA, Aerts HJWL, Andrearczyk V, Apte A, Ashrafinia S, Bakas S, Beukinga RJ, Boellaard R, Bogowicz M, Boldrini L, Buvat I, Cook GJR, Davatzikos C, Depeursinge A, Desseroit MC, Dinapoli N, Dinh CV, Echegaray S, El Naqa I, Fedorov AY, Gatta R, Gillies RJ, Goh V, Götz M, Guckenberger M, Ha SM, Hatt M, Isensee F, Lambin P, Leger S, Leijenaar RTH, Lenkowicz J, Lippert F, Losnegård A, Maier-Hein KH, Morin O, Müller H, Napel S, Nioche C, Orlhac F, Pati S, Pfaehler EAG, Rahmim A, Rao AUK, Scherer J, Siddique MM, Sijtsema NM, Socarras Fernandez J, Spezi E, Steenbakkers RJHM, Tanadini-Lang S, Thorwarth D, Troost EGC, Upadhaya T, Valentini V, van Dijk LV, van Griethuysen J, van Velden FHP, Whybra P, Richter C, Löck S. The Image Biomarker

Standardization Initiative: Standardized Quantitative Radiomics for High-Throughput Image-based Phenotyping. Radiology. 2020 May;295(2):328-338. doi: 10.1148/radiol.2020191145. Epub 2020 Mar 10. PMID: 32154773; PMCID: PMC7193906.

37. Zwanenburg A, Leger S, Vallieres M, Lock S. Image biomarker standardisation initiative. arXiv.org website. https://arxiv.org/abs/1612.07003. Published December 21, 2016. Accessed October 06, 2022

38. Mayerhoefer ME, Materka A, Langs G, Häggström I, Szczypiński P, Gibbs P, Cook G. Introduction to Radiomics. J Nucl Med. 2020 Apr;61(4):488-495. doi: 10.2967/jnumed.118.222893. Epub 2020 Feb 14. PMID: 32060219; PMCID: PMC9374044.

39. Yang F, Wang Y, Li Q, Cao L, Sun Z, Jin J, Fang H, Zhu A, Li Y, Zhang W, Wang Y, Xie H, Gustafsson JÅ, Wang S, Guan X. Intratumor heterogeneity predicts metastasis of triple-negative breast cancer. Carcinogenesis. 2017 Sep 1;38(9):900-909. doi: 10.1093/carcin/bgx071. PMID: 28911002.

40. Sala E, Mema E, Himoto Y, Veeraraghavan H, Brenton JD, Snyder A, Weigelt B, Vargas HA. Unravelling tumour heterogeneity using next-generation imaging: radiomics, radiogenomics, and habitat imaging. Clin Radiol. 2017 Jan;72(1):3-10. doi: 10.1016/j.crad.2016.09.013. Epub 2016 Oct 11. PMID: 27742105; PMCID: PMC5503113.

41. Yip SS, Aerts HJ. Applications and limitations of radiomics. Phys Med Biol. 2016 Jul 7;61(13):R150-66. doi: 10.1088/0031-9155/61/13/R150. Epub 2016 Jun 8. PMID: 27269645; PMCID: PMC4927328.

42. Mu W, Chen Z, Liang Y, Shen W, Yang F, Dai R, Wu N, Tian J. Staging of cervical cancer based on tumor heterogeneity characterized by texture features on (18)F-FDG PET images. Phys Med Biol. 2015 Jul 7;60(13):5123-39. doi: 10.1088/0031-9155/60/13/5123. Epub 2015 Jun 17. PMID: 26083460.

43. Howes OD, McCutcheon R, Agid O, de Bartolomeis A, van Beveren NJ, Birnbaum ML, Bloomfield MA, Bressan RA, Buchanan RW, Carpenter WT, Castle DJ, Citrome L, Daskalakis ZJ, Davidson M, Drake RJ, Dursun S, Ebdrup BH, Elkis H, Falkai P, Fleischacker WW, Gadelha A, Gaughran F, Glenthøj BY, Graff-Guerrero A, Hallak JE, Honer WG, Kennedy J, Kinon BJ, Lawrie SM, Lee J, Leweke FM, MacCabe JH, McNabb CB, Meltzer H, Möller HJ, Nakajima S, Pantelis C, Reis Marques T, Remington G, Rossell SL, Russell BR, Siu CO, Suzuki T, Sommer IE, Taylor D, Thomas N, Üçok A, Umbricht D, Walters JT, Kane J, Correll CU. Treatment-Resistant Schizophrenia: Treatment Response and Resistance in Psychosis (TRRIP) Working Group Consensus Guidelines on Diagnosis and Terminology. Am J Psychiatry. 2017 Mar 1;174(3):216-229. doi: 10.1176/appi.ajp.2016.16050503. Epub 2016 Dec 6. PMID: 27919182; PMCID: PMC6231547.

44. Shi D, Zhang H, Wang G, Yao X, Li Y, Wang S, Ren K. Neuroimaging biomarkers for detecting schizophrenia: A resting-state functional MRI-based radiomics analysis. Heliyon. 2022 Dec 10;8(12):e12276. doi: 10.1016/j.heliyon.2022.e12276. PMID: 36582679; PMCID: PMC9793282.

45. Carrasco-Poves A, Ruiz-Espana S, Brambilla CR, Neuner I, Rajkumar R, Ramkiran S, Lerche C, Moratal D. Analysis of New Biomarkers for the Study of Schizophrenia Following a Radiomics Approach on MR and PET Imaging. Annu Int Conf IEEE Eng Med Biol Soc. 2022 Jul;2022:234-237. doi: 10.1109/EMBC48229.2022.9871543. PMID: 36086347.

46. Nordio G, Easmin R, Giacomel A, et al. An automatic analysis framework for FDOPA PET neuroimaging. Journal of Cerebral Blood Flow & Metabolism. 2023;0(0). doi:10.1177/0271678X231168687

47. K. Friston, “A short history of SPM,” in Statistical Parametric Mapping: The Analysis of Functional Brain Images, 2007, pp. 3–9. doi: 10.1016/B978-012372560-8/50001-2.

48. C. S. Patlak, R. G. Blasberg, and J. D. Fenstermacher, “Graphical evaluation of blood-to-brain transfer constants from multiple-time uptake data.,” J. Cereb. blood flow Metab. Off. J. Int. Soc. Cereb. Blood Flow Metab., vol. 3, no. 1, pp. 1–7, Mar. 1983, doi:10.1038/jcbfm.1983.1.

49. C. S. Patlak and R. G. Blasberg, “Graphical evaluation of blood-to-brain transfer constants from multiple-time uptake data. Generalizations.,” J. Cereb. blood flow Metab. Off. J. Int. Soc. Cereb. Blood Flow Metab., vol. 5, no. 4, pp. 584–590, Dec. 1985,doi: 10.1038/jcbfm.1985.87.

50. Giovanna Nordio, Rubaida Easmin, Alessio Giacomel, Ottavia Dipasquale, Daniel Martins, Steven Williams, Federico Turkheimer, Oliver Howes, Mattia Veronese (2022). Digital data repository and automatic analysis framework for FDOPA PET neuroimaging. 10.1101/2022.04.14.488129.

51. Martinez D, Slifstein M, Broft A, et al. Imaging Human Mesolimbic Dopamine Transmission with Positron Emission Tomography. Part II: Amphetamine-Induced Dopamine Release in the Functional Subdivisions of the Striatum. Journal of Cerebral Blood Flow & Metabolism. 2003;23(3):285-300. doi:10.1097/01.WCB.0000048520.34839.1A

52. Zwanenburg A, Leger S, Agolli L, Pilz K, Troost EG, Richter C, Löck S. Assessing robustness of radiomic features by image perturbation. Scientific reports. 2019 Jan 24;9(1):614.

53. Bettinelli A, Marturano F, Avanzo M, Loi E, Menghi E, Mezzenga E, Pirrone G, Sarnelli A, Strigari L, Strolin S, Paiusco M. A Novel Benchmarking Approach to Assess the Agreement among Radiomic Tools. Radiology. 2022 Jun;303(3):533-541. doi: 10.1148/radiol.211604. Epub 2022 Mar 1. Erratum in: Radiology. 2022 May;303(2):E30. PMID: 35230182.

54. Ligero M, Torres G, Sanchez C, Diaz-Chito K, Perez R, Gil D. Selection of Radiomics Features based on their Reproducibility. Annu Int Conf IEEE Eng Med Biol Soc. 2019 Jul;2019:403-408. doi: 10.1109/EMBC.2019.8857879. PMID: 31945924.

55. Shrout PE, Fleiss JL. Intraclass correlations: uses in assessing rater reliability. Psychol Bull. 1979 Mar;86(2):420-8. doi: 10.1037//0033-2909.86.2.420. PMID: 18839484.

56. Orlhac F, Soussan M, Maisonobe JA, Garcia CA, Vanderlinden B, Buvat I. Tumor texture analysis in 18F-FDG PET: relationships between texture parameters, histogram indices, standardized uptake values, metabolic volumes, and total lesion glycolysis. J Nucl Med. 2014 Mar;55(3):414-22. doi: 10.2967/jnumed.113.129858. Epub 2014 Feb 18. PMID: 24549286.

57. Leger, S., Zwanenburg, A., Pilz, K. *et al.* A comparative study of machine learning methods for time-to-event survival data for radiomics risk modelling. *Sci Rep* **7**, 13206 (2017). https://doi.org/10.1038/s41598-017-13448-3

58. Orlhac F, Boughdad S, Philippe C, Stalla-Bourdillon H, Nioche C, Champion L, Soussan M, Frouin F, Frouin V, Buvat I. A Postreconstruction Harmonization Method for Multicenter Radiomic Studies in PET. J Nucl Med. 2018 Aug;59(8):1321-1328. doi: 10.2967/jnumed.117.199935. Epub 2018 Jan 4. PMID: 29301932.

59. Fortin JP, Cullen N, Sheline YI, Taylor WD, Aselcioglu I, Cook PA, Adams P, Cooper C, Fava M, McGrath PJ, McInnis M, Phillips ML, Trivedi MH, Weissman MM, Shinohara RT. Harmonization of cortical thickness measurements across scanners and sites. Neuroimage. 2018 Feb 15;167:104-120. doi: 10.1016/j.neuroimage.2017.11.024. Epub 2017 Nov 17. PMID: 29155184; PMCID: PMC5845848.

60. Fortin JP, Parker D, Tunç B, Watanabe T, Elliott MA, Ruparel K, Roalf DR, Satterthwaite TD, Gur RC, Gur RE, Schultz RT, Verma R, Shinohara RT. Harmonization of multi-site diffusion tensor imaging data. Neuroimage. 2017 Nov 1;161:149-170. doi: 10.1016/j.neuroimage.2017.08.047. Epub 2017 Aug 18. PMID: 28826946; PMCID: PMC5736019.

61. Koikkalainen J, Hirvonen J, Nyman M, Lötjönen J, Hietala J, Ruotsalainen U. Shape variability of the human striatum--Effects of age and gender. Neuroimage. 2007 Jan 1;34(1):85-93. doi: 10.1016/j.neuroimage.2006.08.039. Epub 2006 Oct 23. PMID: 17056276.

62. Lauer M, Beckmann H. The human striatum in schizophrenia. I. Increase in overall relative striatal volume in schizophrenics. Psychiatry Res. 1997 Feb 7;68(2-3):87-98. doi: 10.1016/s0925-4927(96)02946-0. PMID: 9104756.

63. Roiz-Santiañez R, Suarez-Pinilla P, Crespo-Facorro B. Brain Structural Effects of Antipsychotic Treatment in Schizophrenia: A Systematic Review. Curr Neuropharmacol. 2015;13(4):422-34. doi: 10.2174/1570159x13666150429002536. PMID: 26412062; PMCID: PMC4790397.

64. Gutman BA, van Erp TGM, Alpert K, Ching CRK, Isaev D, Ragothaman A, Jahanshad N, Saremi A, Zavaliangos-Petropulu A, Glahn DC, Shen L, Cong S, Alnaes D, Andreassen OA, Doan NT, Westlye LT, Kochunov P, Satterthwaite TD, Wolf DH, Huang AJ, Kessler C, Weideman A, Nguyen D, Mueller BA, Faziola L, Potkin SG, Preda A, Mathalon DH, Bustillo J, Calhoun V, Ford JM, Walton E, Ehrlich S, Ducci G, Banaj N, Piras F, Piras F, Spalletta G, Canales-Rodríguez EJ, Fuentes-Claramonte P, Pomarol-Clotet E, Radua J, Salvador R, Sarró S, Dickie EW, Voineskos A, Tordesillas-Gutiérrez D, Crespo-Facorro B, Setién-Suero E, van Son JM, Borgwardt S, Schönborn-Harrisberger F, Morris D, Donohoe G, Holleran L, Cannon D, McDonald C, Corvin A, Gill M, Filho GB, Rosa PGP, Serpa MH, Zanetti MV, Lebedeva I, Kaleda V, Tomyshev A, Crow T, James A, Cervenka S, Sellgren CM, Fatouros-Bergman H, Agartz I, Howells F, Stein DJ, Temmingh H, Uhlmann A, de Zubicaray GI, McMahon KL, Wright M, Cobia D, Csernansky JG, Thompson PM, Turner JA, Wang L. A meta-analysis of deep brain structural shape and asymmetry abnormalities in 2,833 individuals with schizophrenia compared with 3,929 healthy volunteers via the ENIGMA Consortium. Hum Brain Mapp. 2022 Jan;43(1):352-372. doi: 10.1002/hbm.25625. Epub 2021 Sep 8. PMID: 34498337; PMCID: PMC8675416.

65. Taylor S, Christensen JD, Holcomb JM, Garver DL. Volume increases in striatum associated with positive symptom reduction in schizophrenia: a preliminary observation. Psychiatry Res. 2005 Oct 30;140(1):85-9. doi: 10.1016/j.pscychresns.2005.06.004. Epub 2005 Sep 27. PMID: 16194599.

66. Mendrek A, Mancini-Marïe A. Sex/gender differences in the brain and cognition in schizophrenia. Neurosci Biobehav Rev. 2016 Aug;67:57-78. doi: 10.1016/j.neubiorev.2015.10.013. Epub 2015 Dec 30. PMID: 26743859.

67. Canuso CM, Pandina G. Gender and schizophrenia. Psychopharmacol Bull. 2007;40(4):178-90. PMID: 18227787.

68. Maltais JR, Gagnon G, Garant MP, Trudel JF. Correlation between age and MMSE in schizophrenia. Int Psychogeriatr. 2015 Nov;27(11):1769-75. doi: 10.1017/S1041610215000459. Epub 2015 Apr 15. PMID: 25872525.

69. Baron JC, Martinot JL, Cambon H, Boulenger JP, Poirier MF, Caillard V, Blin J, Huret JD, Loc'h C, Maziere B. Striatal dopamine receptor occupancy during and following withdrawal from neuroleptic treatment: correlative evaluation by positron emission tomography and plasma prolactin levels. Psychopharmacology (Berl). 1989;99(4):463-72. doi: 10.1007/BF00589893. PMID: 2574481.

70. Park JE, Kim HS. Radiomics as a Quantitative Imaging Biomarker: Practical Considerations and the Current Standpoint in Neuro-oncologic Studies. Nucl Med Mol Imaging. 2018 Apr;52(2):99-108. doi: 10.1007/s13139-017-0512-7. Epub 2018 Feb 1. PMID: 29662558; PMCID: PMC5897262.